1. Introduction

Laboratory studies on the chemistry of the atmosphere are of great importance for understanding and providing scientific basis for the mitigation of such grave environmental problems as the depletion of the Earth's protecting ozone layer, acidic rains and deterioration of the quality of air. In connection with the latter, it is of particular concern that the frequency of urban smog has recently increased substantially as an effect of global warming.

The oxygenated organic molecules (OVOs) play a very important role in the chemistry of the troposphere. During their degradation reactive free radicals are formed which basically affect the oxidation capacity, the concentration of ozone and $^{\bullet}$OH-radicals as well as the transformations of nitrogen-oxides in the atmosphere. OVOs have natural and anthropogenic sources (vegetation, industry, traffic) and are formed in greater part via the oxidation of hydrocarbons. The initial steps in the atmospheric depletion of aliphatic aldehydes and ketones are their reactions with the $^{\bullet}$OH-radicals and photolysis. Accordingly, in my PhD work I have studied the kinetics of the $^{\bullet}$OH-reactions and photolysis processes. The free radicals, formed in these reactions react exclusively with O_2 in the troposphere. Thus a major subject of my work was also the study of the reactions of acyl-radicals with O_2. The motivation, approaches and immediate goals of my investigations have been basic research. I have addressed such questions of fundamental scientific interest, as for instance, the kinetics of overall reactions, product branching ratios, energy transfer from electronically excited molecules by collisions, connections between molecular structure and reactivity, etc. On the other hand, the laboratory results have been utilised in atmospheric modelling studies. The chemical and photochemical changes in the atmosphere are described and investigated by sophisticated atmospheric chemistry models. The reliability of these models is basically determined by the accuracy of the kinetic and photochemical parameters of the elementary processes that comprise the complex mechanisms.

The following reactions have been investigated in my PhD work:

$CH_3C(O)CH_3 + h\upsilon \longrightarrow$ products	(1)	$-\Phi_{Ac}$
$\longrightarrow CH_3{}^{\bullet}CO + {}^{\bullet}CH_3$	(1a)	
$CH_3C(O)CH_2CH_3 + h\upsilon \longrightarrow$ products	(2)	$-\Phi_{MEK}$
$\longrightarrow CH_3{}^{\bullet}CO + {}^{\bullet}CH_3CH_2$	(2a)	
$CH_3{}^{\bullet}CO + O_2 \longrightarrow$ products	(3)	$-\Gamma_{3b} = k_{3b} / k_3$
$CH_3{}^{\bullet}CO + O_2 + M \longrightarrow CH_3C(O)OO^{\bullet} + M$	(3a)	
$\longrightarrow {}^{\bullet}OH +$ products	(3b)	
$CH_3CH_2{}^{\bullet}CO + O_2 \longrightarrow$ products	(4)	$-\Gamma_{4b} = k_{4b} / k_4$
$CH_3CH_2{}^{\bullet}CO + O_2 + M \longrightarrow CH_3CH_2C(O)OO^{\bullet} + M$	(4a)	
$\longrightarrow {}^{\bullet}OH +$ products	(4b)	
${}^{\bullet}OH + CH_3C(O)H \longrightarrow$ products	(5)	$-k_5$
${}^{\bullet}OH + CH_3CH_2C(O)H \longrightarrow$ products	(6)	$-k_6$
${}^{\bullet}OH + CH_3C(O)Cl \longrightarrow$ products	(7)	$-k_7$

Photodissociation quantum yields (Φ_{Ac} and Φ_{MEK}), $^{\bullet}$OH-product yields (Γ_{3b} and Γ_{4b}), as well as rate coefficients for $^{\bullet}$OH-reactions (k_5–k_7) were determined in my experiments. The photolysis mechanism suggested for aliphatic ketones in the literature has been validated and further elaborated. The temperature dependence of the absorption cross-section of methyl-ethyl-ketone, σ_{MEK}, has also been determined.

2. Experimental

The subjects of my PhD Thesis are photochemical processes and the kinetics of gas-phase elementary reactions. Thus, I have applied essentially two types of experimental methods: pulsed-laser photolysis (LF) and the fast discharge-flow reaction kinetic technique (DF).

The photodissociation quantum yields (Φ_{Ac} és Φ_{MEK}) were determined by using exciplex-laser photolysis coupled with gas-chromatographic measurements of the concentration depletion of acetone and MEK. The photolysis experiments were carried out in a thermostated quartz reactor; the reaction mixture, beside acetone, contained synthetic air buffer gas and GC internal standard. Samples were taken at regular time intervals with gas-tight syringe, the number of laser shots (the reaction time) was recorded and the laser energy per pulse was measured. The quantum yields were calculated by the concentration depletion and the absorbed laser energy.

The absorption cross-sections are also needed for obtaining the quantum yields. For the determination of UV-absorption spectra and the measurement of temperature dependence I have developed, optimised and tested a new gas-spectrophotometer. A special feature of this equipment is that it can be operated under flow-through conditions which has been found to be very important in the low-temperature measurements to avoid wall-absorptions.

Reaction rate constants (k_5-k_7) and $^{\bullet}$OH-product yields (Γ_{3b} és Γ_{4b}) have been determined by applying the DF method, which is suitable for the "direct" investigation of elementary reactions at the ms time scale. The main part of the apparatus is a flow reactor, which is equipped with a movable injector. The OH radicals were produced inside the injector by reacting F atoms with H_2O or H atoms with NO_2 ; atoms were obtained by microwave discharge. The reactants highly diluted with He, were introduced upstream through a side arm into the reactor. At the given linear flow-rate, the reaction time is set by the distance between the distance of the tip of the injector and the detection block. $^{\bullet}$OH-radicals were monitored at the end of the flow tube by using the sensitive and selective detection methods of resonance fluorescence (RF) and laser induced fluorescence (LIF). The light source for RF excitation was an $^{\bullet}$OH-lamp which was operated by microwave discharge of H_2O vapour (excitation and observation: 308 nm). A Nd:YAG-pumped frequency-doubled dye laser was used for the LIF detection (excitation: 282 nm, observation: 308 nm). The experiments were carried out under pseudo-first-order conditions.

3. Results

I. Temperature- and pressure dependence of the photodissociation quantum yield of acetone and methyl-ethyl-ketone

The photodissociation quantum yield (QY) of acetone and methyl-ethyl-ketone has been determined in synthetic air at 308 nm photolysis wavelength, in the temperature- and pressure ranges of T = 233 - 323 K and P = 13 - 998 mbar, respectively. QYs were determined by measuring the depletion of the concentration of the two ketones with GC analysis. The experimental data have been evaluated by applying equation (1) which was derived previously in our research group:

$$\ln ([Ac]_n / [Ac]_0) = -(\alpha \cdot \sigma_{Ac}(308\ \text{nm}, T) \cdot \Phi_{Ac}(308\ \text{nm}, p, T) \cdot (n \cdot E) \qquad (1)$$

where $[Ac]_0$ and $[Ac]_n$ designate the initial concentration of acetone and that remaining after n laser shots, α is a known constant, σ_{Ac} is the absorption cross section of acetone and E is the laser energy by pulse. One of the typical diagrams used for the evaluations of the experimental data are presented as an insert in Fig. 1. The photodissociation quantum yields of both acetone and methyl-ethyl-ketone have been found to decrease with decreasing temperature and to decrease also with increasing pressure. As for instance, Φ_{Ac} and Φ_{MEK} decrease about 70 % and 50 %, respectively when one decrease the temperature from 323 K to 233 K (Table 1.)

	***P* (298 K) / mbar**	**323 K**	**298 K**	**273 K**	**253 K**	**233 K**
Acetone	133	0,368 ± 0,002	0,319 ± 0,032	0,228 ± 0,002	0,178 ± 0,010	0,122 ± 0,014
MEK	133	0,831 ± 0,001	0,817 ± 0,001	0,518 ± 0,001	0,463 ± 0,042	0,416 ± 0,003
Acetone	998	0,145 ± 0,040	0,112 ± 0,008	0,046 ± 0,006	0,036 ± 0,002	–
MEK	998	0,336 ± 0,030	0,294 ± 0,017	0,174 ± 0,001	0,155 ± 0,001	–

Table 1. *The temperature- and pressure dependence of the photodissociation quantum yield of acetone and MEK presented at two pressures.*

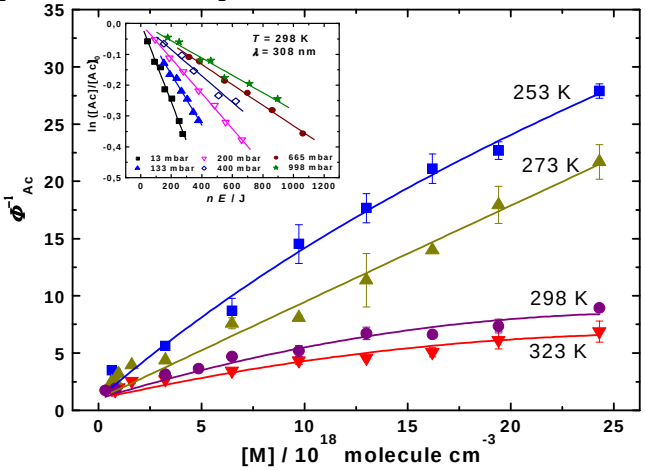

Figure 1. *Stern-Volmer (SV) plots for the photodecomposition QY of acetone at λ = 308 nm photolysis wavelength in synthetic air. The semilogarithmic decay plots in the insert show typical results of the evaluation of the experimental data according to eq. (1) to obtain Φ_{Ac}.*

In the greater part of the pressure range studied, the *P*-dependence of QYs display linearity for both ketones in SV-plots, at low pressures, however some “curvature” of the plots is observed (see Fig. 1.). A photolysis mechanism has been proposed in accordance with the

experimental findings in which the photodissociation occurs from two excited states ($R^{\bullet}$ = $^{\bullet}CH_3$ – acetone, $R^{\bullet}$ = $^{\bullet}C_2H_5$ – MEK):

$S_0 + h\nu \rightarrow S_1$	I_a
$S_1 \rightarrow CH_3{}^{\bullet}CO + R^{\bullet}$	k_{RS}
$S_1 + M \rightarrow S_0 + M$	k_{QS}
$S_1 \rightarrow T_1$	k_{ISC}
$T_1 \rightarrow CH_3{}^{\bullet}CO + R^{\bullet}$	k_{RT}
$T_1 + M \rightarrow S_0 + M$	k_{QT}

In the mechanism S_0, S_1 and T_1 designate the ground state, the first excited singlet state and the first excited triplet state of acetone, respectively. k_{RS}, k_{QS}, k_{ISC}, k_{RT} és k_{QT} are the rate coefficients of the respective elementary steps and I_a is the rate of light absorption. Product formation occurs from both the S_1 and T_1 states and both states can undergo physical quenching as well. Decrease of the quantum yields with pressure (with the increase of the concentration of the buffer-gas) indicates that physical quenching of the electronically excited molecules compete with their unimolecular dissociation. Equation (2) can be derived by the mechanism; curve-fitting to the experimental data have returned the parameters a_1, a_2 and a_3 (the estimated curves are shown in the main panel of Fig. 1)

$$\Phi^{-1} = \frac{\left(1 + a_2 + a_1[\mathrm{M}]\right)\left(1 + a_3[\mathrm{M}]\right)}{\left(1 + a_3[\mathrm{M}] + a_2\right)},\ a_1 = \frac{k_{QS}}{k_{RS}},\ a_2 = \frac{k_{ISC}}{k_{RS}},\ a_3 = \frac{k_{QT}}{k_{RT}}. \qquad (2)$$

At high buffer-gas concentrations eq. (2) simplifies to the linear form:

$$\Phi^{-1} = (1 + a_2 + a_1\,[\mathrm{M}]) \qquad (3)$$

Because of technical reasons, in the low-pressure region I could perform only a few experiments and so the results of the parameter estimations are very uncertain for the initial part of the SV plots. In contrast, at higher pressures (above about 130 mbar, $[M] \geq 3 \cdot 10^{18}$ molecule $\cdot$ cm^{-3}), where most of the experiments were carried out, the Stern-Volmer plots showed good linearity. Therefore, the results of linear fittings were considered in the discussions.

T / K	**a_1 (= k_{QS}/k_{RS}) / 10^{19} cm^3 · molecule^{-1}**	
	Acetone	**MEK**
233	–	3,24 ± 0,587
253	10,7 ± 0,255	2,09 ± 0,266
273	7,35 ± 0,057	1,74 ± 0,002
298	2,73 ± 0,122	1,04 ± 0,075
323	1,97 ± 0,132	0,59 ± 0,028

Table 2. *Results of the 2-parameter estimations to the [M] – Φ^{-1} experimental data according to eq. (3) which is based on proposed photolysis mechanism.*

Parameter a_1 (= k_{QS}/k_{RS}) decreases with temperature for both acetone and MEK (Table 2.). The probable reason on this temperature dependence is that product formation from the S_1 state occurs through reaction barrier and so the constant k_{RS} increases with increasing temperature. The following barrier heights have been estimated by employing an empirical Arrhenius expression: $E_{S1,Ac}$ = 295 ± 7 nm = 406 ± 10 kJ $\cdot$ mol^{-1} (acetone),

$E_{S1,MEK}$ = 300 ± 5 nm = 398 ± 7 kJ $\cdot$ mol^{-1} (methyl-ethyl-ketone).

II. Temperature dependence of the absorption spectrum of methyl-ethyl-ketone

The temperature dependence of the absorption cross-section of methyl-ethyl-ketone has been determined in my PhD work the first time (λ = 220-350 nm; T = 253-363 K). Measurements of the spectra were taken with a slowly flowing MEK samples through the thermostated absorption cell. The absorbance was measured at different methyl-ethyl-ketone concentrations and σ_{MEK} was obtained by the Lambert-Beer low. The absorption cross section has been found to have significant T-dependence (Fig. 2). As for instance σ_{MEK} increases at 308 nm by about 60 % when increasing the temperature from 253 K to 363 K.

253 K	273 K	298 K	323 K	343 K	363 K
1,459 ± 0,267	1,688 ± 0,015	1,885 ± 0,028	2,031 ± 0,001	2,131 ± 0,001	2,334 ± 0,001

Table 3. *The absorption cross-section of methyl-ethyl-ketone at 308 nm and different temperatures (in 10^{-20} $cm^2 \cdot molecule^{-1}$units).*

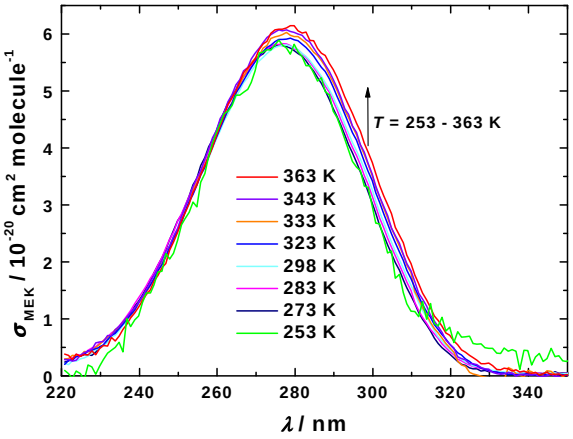

Figure 2. *The UV-absorption spectrum of methyl-ethyl-ketone at different temperatures.*

III. Reactions of acetyl ($CH_3CO^{\bullet}$) and propionyl ($C_2H_5CO^{\bullet}$)radicals with O_2

Kinetics of the reactions were studied by applying the fast discharge flow experimental technique. We could not detect the acyl radicals in our experiments, but strong $^{\bullet}$OH-signals were observed which allowed the kinetics of the reactions to be studied and an accurate determination of the $^{\bullet}$OH-product yields. The observation was that the $^{\bullet}$OH-signals increased very substantially when O_2 was added to the reactions $^{\bullet}$OH + acetaldehyde and $^{\bullet}$OH + propionaldehyde. This has indicated the reformation of $^{\bullet}$OH in the reaction system through chemical chain reactions, a schematics for which is shown below for the acetyl + O_2 reaction:

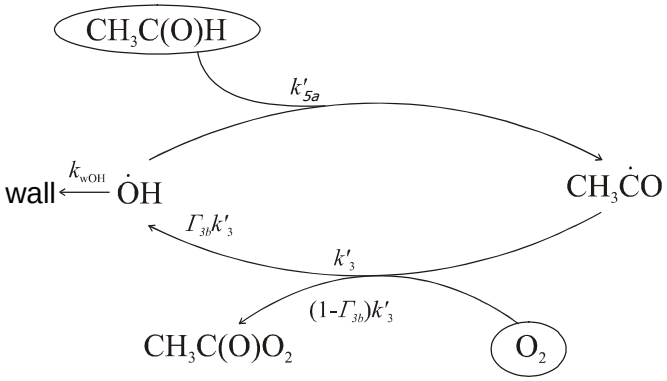

Figure 3. *Reformation of $^{\bullet}$OH in the CH_3CO + O_2 reaction system. $\Gamma_{3b} = k_{3b} / k_3$, $k'_3 = k_3 \cdot [O_2]$, $k'_{5a} = k_{5a} \cdot [CH_3C(O)H]$.*

An analytical solution can be given for the differential-equation system of the reactions, the final results of which are the following simple expressions:

$$\Gamma_{3b} = \frac{\kappa_{0,3} - \kappa_3^*}{\kappa_{0,3} - k_{wOH,3}} \text{ and } \Gamma_{4b} = \frac{\kappa_{0,4} - \kappa_4^*}{\kappa_{0,4} - k_{wOH,4}}, \qquad (4)$$

where κ_0 and κ^* designate the $^{\bullet}$OH-decay constants determined in the experiments in the presence and absence of O_2, respectively and , k_{wOH} stands for the rate coefficient of the $^{\bullet}$OH-loss on the wall of the reactors.

In Fig. 4., characteristic $^{\bullet}$OH-consumption curves are presented with and without added O_2. As seen in the inserted figure, the time variation of the concentration of $^{\bullet}$OH radicals obeys first order kinetics: the semilogarithmic plots give lines.

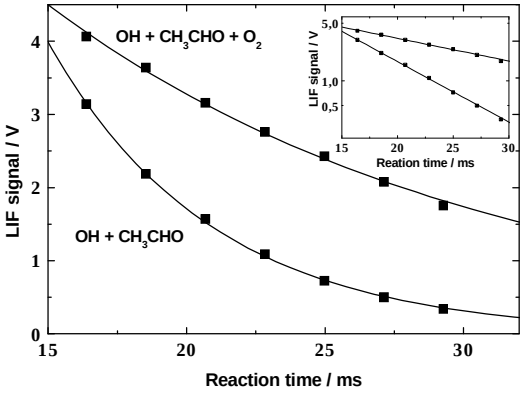

Figure 4. *Representative $^{\bullet}$OH-decay profiles determined in the presence and absence of O_2 for the $CH_3CO + O_2$ reaction system (P = 3,33 mbar, T = 298 K).*

Large $^{\bullet}$OH branching ratios (yields) have been observed for both reactions at the low pressures of the experiments. The $^{\bullet}$OH-yields are close to unity at around 1 mbar, but decrease strongly with pressure (Fig. 5.).

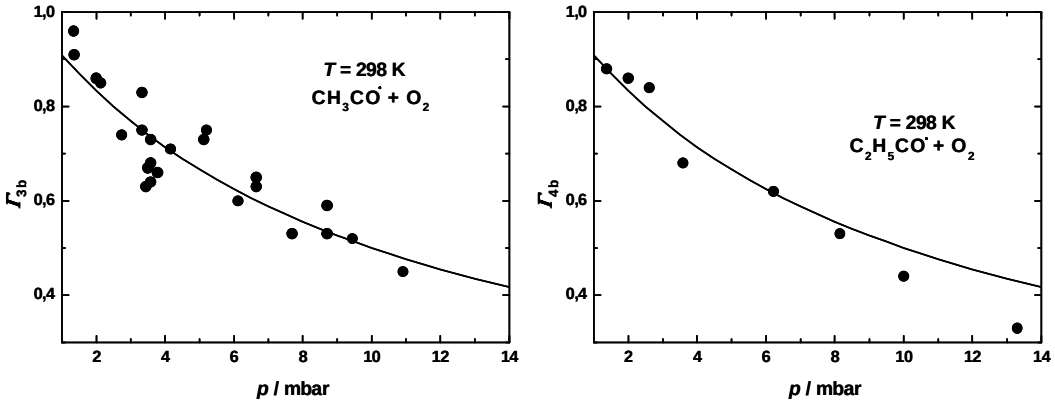

Figure 5. *Pressure dependence of the $^{\bullet}$OH product yield for the reactions of acetyl and propionyl radicals with O_2 at room temperature in He buffer gas.*

The pressure dependence can be explained by the Lindemann-Hinshelwood formalism. Accordingly a chemical-activation reaction takes place, where in the association step a vibrationally excited peroxy radical is formed which can either reform the reactants, can be stabilised by collisions, moreover it can undergo reaction to form $^{\bullet}$OH-radicals:

$R^{\bullet}CO + O_2 \rightarrow (RC(O)OO^{\bullet})^*$ (A)

$(RC(O)OO^{\bullet})^* \rightarrow R^{\bullet}CO + O_2$ (–A)

$(RC(O)OO^{\bullet})^* + M \rightarrow (RC(O)OO^{\bullet}) + M$ (Q)

$(RC(O)OO^{\bullet})^* \rightarrow {}^{\bullet}OH + X$ (B)

The above scheme is valid for both the acetyl radical + O_2 and propionyl radical + O_2 reactions. R designates CH_3 or C_2H_5 groups, the star refers to vibrational excitation, M is the third-body colliding partner and X designate the other products beside $^{\bullet}$OH.
The following expression is derived for the $^{\bullet}$OH-yields:

$$\Gamma_{3b} = \frac{k_B}{k_B + k_Q[M]} \text{ , similarly } \Gamma_{4b} \text{ is.} \qquad (5)$$

Equation (5) is in accordance with the observation that the $^{\bullet}$OH-yield is close to unity at low pressures and approaches zero at high pressures.

III. Kinetics of the reactions of $^{\bullet}$OH-radicals with Organic molecules

Reactions of $^{\bullet}$OH with acetaldehyde and propionaldehyde

The overall rate constants for the acetaldehyde and propionaldehyde reactions, k_5 and k_6, could be obtained from the κ_0 values which were determined in connection with the $^{\bullet}$OH-yield studies. This is because κ_0 in equation (4) is in fact the "pseudo-first-order" rate coefficient: $\kappa_{0,3} = k'_5 = k_5 \cdot [CH_3C(O)H]$ and $\kappa_{0,4} = k'_6 = k_6 \cdot [C_2H_5C(O)H]$. The pseudo-first-order rate coefficients plotted against the aldehyde concentrations provided straight lines in a wide concentration range (Fig. 6), the slopes give the bimolecular rate constants:

$$k_5(298\text{ K}) = (1{,}25 \pm 0{,}09) \cdot 10^{-11}\ \text{cm}^3 \cdot \text{molecule}^{-1} \cdot \text{s}^{-1},$$
$$k_6(298\text{ K}) = (1{,}85 \pm 0{,}06) \cdot 10^{-11}\ \text{cm}^3 \cdot \text{molecule}^{-1} \cdot \text{s}^{-1}.$$

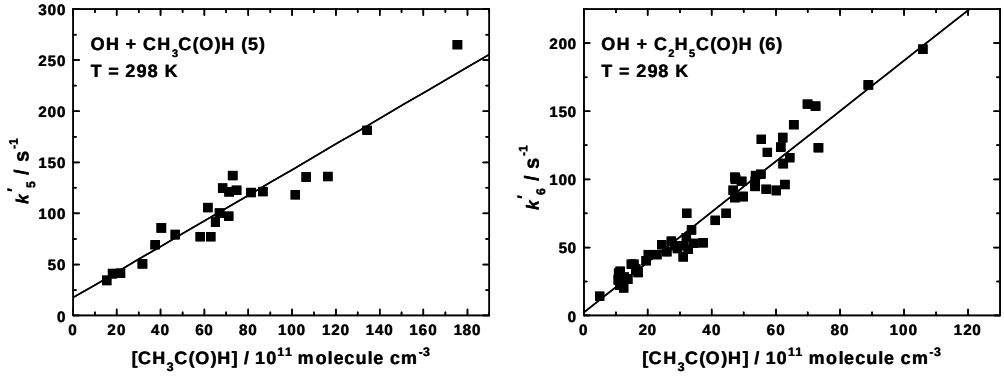

Figure 6. *Plots of pseudo-first-order rate constants vs. the aldehyde concentrations.*

The reaction of acetyl-cloride with $^{\bullet}$OH radicals

The kinetics of the reaction (7) were investigated with DF/RF by using so called "on-off" experimental technique. At given position of the injector (i.e. at given reaction distance, Δz) the $^{\bullet}$OH signal strengths were recorded in the presence (S_{on}) and absence (S_{off}) of the reactants. The pseudo-first-order rate constant, $k'_7 = k_7\,[CH_3C(O)Cl]$, was obtained by means of equation (6):

$$-\ln \frac{S_{on}}{S_{off}} = k'_7 \cdot \frac{\Delta z}{v_{lin}} \qquad (6)$$

where v_{lin} is the linear flow rate in the reactor. The insert of Fig. 7. shows typical $^{\bullet}$OH-decays in semilogarithmic plots, the main panel presents k'_7 vs. $[CH_3C(O)Cl]$, the slope of the straight lines gives: $k_7(298\text{ K}) = (1{,}70 \pm 0{,}07) \cdot 10^{-14}\ \text{cm}^3 \cdot \text{molecule}^{-1} \cdot \text{s}^{-1}$.

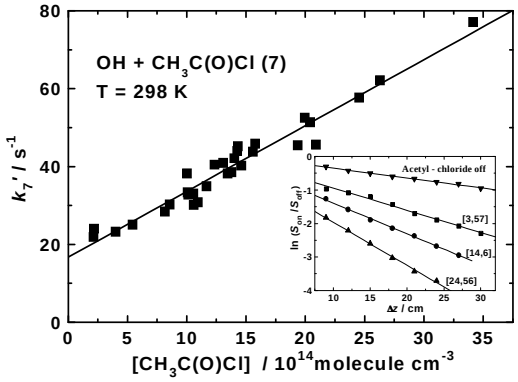

Figure 7. *Plot of the pseudo-first-order rate constant vs. the acetyl-chloride concentration. The insert shows results according to eq. (6); in bracets $CH_3C(O)Cl$ concentrations are given in 10^{14} molecule · cm^{-3}.*

In Table 4., the rate coefficients of the ˙OH-reactions have been summerised that I have investigated in my PhD work.. Large differences are seen in the reactivities: ˙OH reacts much faster with the aldehydes than does with acetyl-chloride. This is understood by the low dissociation energy of the carbonyl RC(O)–H bond on one hand, and, on the other hand by the negative inductive effect of the Cl-substituent. Consequently, both the thermochemistry and inductive effects have to be considered in order to explain the reaction kinetic properties of ˙OH-reactions.

Reaction (*i*)	k_i **/ molecule · cm^{-3} · s^{-1}**	k_5 / k_i
OH + $CH_3C(O)H$ (5)	$(1{,}25 \pm 0{,}09) \cdot 10^{-11}$	1
OH + $C_2H_5C(O)H$ (6)	$(1{,}85 \pm 0{,}06) \cdot 10^{-11}$	0,7
OH + $CH_3C(O)Cl$ (7)	$(1{,}70 \pm 0{,}07) \cdot 10^{-14}$	735

Table 4. *Comparison of the rate coefficients of the studies ˙OH-reactions.*

4. New scientific results

1. The photodissociation quantum yield of acetone decreases significantly with decreasing temperature and with increasing pressure (λ = 308 nm, T = 233 - 323 K, p = 13 - 998 mbar, synthetic air). The quantum yields in Stern-Volmer (SV) plots (Φ_{Ac}^{-1} – [M]). At [M] > $3 \cdot 10^{18}$ molecule $\cdot$ cm^{-3} buffer gas concentration display straight lines, while in the low pressure region the data points lie below the straight lines. The SV plots indicate that the photodecomposition occurs from at least two electronically excites states, which are pressure quenched by different efficiency. By results have contributed to help resolve the disparity in the literature. [2], [3].

2. The photolysis quantum yields of methyl-ethyl-ketone similarly – to those of acetone – exhibit positive temperature dependence and also decrease with pressure (λ = 308 nm, T = 233 - 323 K p = 67 - 998 mbar, synthetic air). The Stern-Volmer plots are linear in the pressure range studied. The photodissociation quantum yield of methyl-ethyl-ketone is significantly larger than that of acetone, however it shows less pronounced temperature dependence. The quantum yield for methyl-ethyl-ketone photodissociation has been determined in my PhD work the first time under conditions relevant to the atmosphere. [6].

3. The photolysis of acetone and methyl-ethyl-ketone can both be described by essentially the same mechanism. In this mechanism photodissociation may take place from both the first excited singlet (S_1) and the first excited triplet (T_1) states. Physical quenching by collisions compete with the unimolecular dissociation and the quenching is stronger in the case of the triplet molecules. A 3-parameter relationship derived by the mechanism describes well the temperature- and pressure dependence of the SV plots. The 3 parameters supply rate coefficient ratios for the elementary steps comprising the mechanism. The ratio of the quenching rate coefficient of the S_1 state (k_{QS}) and that of the unimolecular decomposition from the singlet state (k_{RS}) decreases with increasing temperature. This may be taken as an indication for that the photodissociation on the S_1 potencial surface occurs through energy barrier. By the analysis of the temperature dependence the following values have been estimated for the barrier heights: acetone: $E_{S1,Ac}$ = 295 ± 7 nm = 406 ± 10 kJ $\cdot$ mol^{-1}, methyl-ethyl-ketone: $E_{S1,MEK}$ = 300 ± 5 nm = 398 ± 7 kJ $\cdot$ mol^{-1}. [3], [6].

4. The absorption spectrum of methyl-ethyl-ketone shows slight positive temperature dependence which is, however, non-negligible from an atmospheric chemistry point of view. As for instance at 308 nm, increasing the temperature from 253 K to 363 K, the absorption cross-section increases by as much as 60 %. No temperature dependent absorption spectrum for MEK has been reported previously. [6].

5. At a few mbar pressures $^{\bullet}$OH-radicals are the main products in the reactions $CH_3CO^{\bullet}$ + O_2 and $C_2H_5CO^{\bullet}$ + O_2 in contrast with the previous view that only peroxy radicals are formed in the reactions. The branching ratio for $^{\bullet}$OH formation ($\Gamma_{3b} = k_{3b} / k_3$, $\Gamma_{4b} = k_{4b} / k_4$) is close to unity at around 1 mbar of pressure, but the $^{\bullet}$OH-yields decrease strongly with pressure. The observed pressure dependence can be understood by the occurrence of a chemical-activation mechanism, in which vibrationally excited peroxy redicals are formed which can be stabilised by collisions, can revert to the reactants or undergo reaction to form $^{\bullet}$OH-radicals. [4], [5].

6. New rate coefficient values at room temperature have been determined by means of the thermal DF method for the reactions $^{\bullet}$OH + $CH_3C(O)H$ (5) and $^{\bullet}$OH + $C_2H_5C(O)H$ (6): k_5(298 K) = (1,25 ± 0,09) $\cdot$ 10^{-11} and k_6(298 K) = (1,85 ± 0,06) $\cdot$ 10^{-11} cm^3 $\cdot$ molecule^{-1} $\cdot$ s^{-1}.

[5]. These rate coefficient values agree well with those reported in the literature by photolytic experiments.

7. The first rate coefficient has been determined in my work by using a direct reaction kinetic method (DF/RF) for the reaction of $^{\bullet}$OH-radical with acethyl-chloride: $k_7(298\ K) = (1{,}70 \pm 0{,}07) \cdot 10^{-14}\ cm^3 \cdot molecule^{-1} \cdot s^{-1}$. [1]. The most recent critical reaction kinetics data evaluation by IUPAC recommends this value from my experiments for use, e.g. for the purpose of atmospheric modelling studies.

5. Possible practical applications

Our research group has joined the EU's SCOUT-O3 atmospheric chemistry project in 2004. In this project there are participants from 19 countries in 59 institutions. The main objective to SCOUT-O3 has been to provide predictions about the future of the chemistry of the atmosphere with special emphasis on the interplay between atmospheric chemistry and climate change. The focus of research has been on the concentration of ozone in the upper troposphere and lower stratosphere as well as the changes in UV radiation and its effect on global warming.

Participants of the project have been performing field measurements, computer modelling and laboratory investigations. In my PhD work I have determined important parameters for use as input data in the models. Such are the photodossociation quantum yields, the temperature and pressure dependence, as well as the rate coefficients for OH-reactions. Part of my results have already been utilised in the modelling studies: it has been concluded that application of temperature dependent acetone QYs have resulted in substantial effects revealing the role of acetone photolysis to be significantly less important in the chemistry of the atmosphere, than it was thought before. This new modelling results indicates that the whole atmospheric budget of acetone has to be re-evaluated.

6. List of scientific publication

Publications directly related to the PhD thesis

1. Rate constant for the reaction of OH radicals with $CH_3C(O)Cl$ determined by direct kinetic method, R. Nádasdi, I. Szilágyi, Gg. Kovács, S. Dóbé, T. Bérces, F. Márta, *React. Kinet. Catal. Letters*, 89, 193-199, 2006. (IF: 0,514, I: 2)

2. Determination of the photolysis puantum yield of 2-butanone and acetone-d_6 by using exciplex-laser photolysis, R. Nádasdi, *Period. Politech.*, 51 (2), 98, 2006. (IF: 0, I: 0)

3. Exciplex laser photolysis study of acetone with relevance to tropospheric chemistry,
R. Nádasdi, Gg. Kovács, I. Szilágyi, A. Demeter, S. Dóbé, T. Bérces, F. Márta, *Chem. Phys. Letters*, 440, 31-35, 2007. (IF: 2,481, I: 3)

4. Kinetics and mechanism of the reactions of CH_3CO and $CH_3C(O)CH_2$ radicals with O_2. Low-pressure discharge flow experiments and quantum-chemical computations,
Gg. Kovács, J. Zádor, E. Farkas, R. Nádasdi, I. Szilágyi, S. Dóbé, T. Bérces, F. Márta, Gy. Lendvay, *Phys. Chem. Cem. Phys.*, 9, 4142-4154, 2007. (IF: 2,898, I: 3)

5. Experimental and theoretical study of the reactions $C_2H_5CO + O_2$ and $CH_3CHC(O)H + O_2$, R. Nádasdi, I. Szilágyi, G. L. Zügner, S. Dóbé, J. Zádor, X. Song and B. Wang, *Proceedings of the European Combustion Meeting ECM 2009.* (közlésre elfogadva, 2009, február 2.) (IF: 0, I: 0)

6. Photolysis quantum yield and UV absorption spectrum for methyl-ethyl-ketone, R. Nadasdi, G. L. Zügner, M. Farkas, S. Dóbé, E. Szabó, A. Tomas, C. Fittschen, *J. Photochem. Photobiol. A: Chemistry*, (közlésre előkészítve, a benyújtás várható ideje: 2009. 03. 15.).

Other publications directly related to the PhD thesis

7. Rate constant for the reaction of bromine atoms with ethane: kinetic and thermochemical implications, G. L. Zügner, I. Szilágyi, R. Nádasdi, J. Zádor and S. Dóbé, *React. Kinet. Catal. Letters*, 95., 355-363, 2008. (IF: 0,587, I: 0)

8. Competitive bromination kinetic study of C_2H_6, CH_2ClBr and neo-C_5H_{12}. Reaction kinetics and thermochemical implications, R. Nádasdi, I. Szilágyi, J. Zádor, G. Zügner, S. Dóbé, T. Bérces, F. Márta, *Proceedings of the European Combustion Meeting ECM 2007*, 111–114, 2007. (IF: 0, I: 0)

Presentations

1. 2-butanon és aceton-D_6 fotobomlási kvantumhatásfokának meghatározása exciplex-lézer fotolízissel, Nádasdi Rebeka, *Doktoráns Konferencia BME*, Budapest, 2006 február 7, (előadás).

2. Vízgőz hatásának vizsgálata az aceton fotobomlási kvantumhatásfokára exciplex-lézer fotolízissel, Nádasdi Rebeka, *MTA Reakciókinetikai és Fotokémiai Munkabizottsági ülése*, Balatonalmádi, 2007 április 26, (előadás).

3. Vízgőz hatásának vizsgálata az aceton fotobomlási kvantumhatásfokára exciplex-lézer fotolízissel, Nádasdi Rebeka, Anyag és Környezetkémiai Intézeti Szeminárium, 2007 március 13, (előadás).

4. OH - gyök képződés a CH_3CO - és C_2H_5CO - gyökök O_2 molekulával végbemenő gázfázisú elemi reakciójában, Nádasdi Rebeka, *XI. Doktori Kémiai Iskola*, MTA KK, 2008 április 21-22, (előadás).

5. Overall kinetics and products study for the reactions of CH_3CO and $CH_3C(O)CH_2$ radicals with O_2, R. Nádasdi, E. Farkas, Gg. Kovács, J. Zádor, S. Dóbé, T. Bérces, F. Márta, *19th International Symposium on Gas Kinetics*, Orleans, 2006 július 22-27, (poszter).

6. Chemistry-climate coupling: Laboratory kinetics and photochemical studies of key atmospheric carbonyls, S. Dóbé, R. Nádasdi, Gg. Kovács, J. Zádor, T. Bérces, F. Márta, *1st Euchem*, Budapest, 2006 augusztus 27-31, (poszter).

7. Photolysis quantum yields for acetone and methyl-ethyl-ketone, Gg. Kovács, R. Nádasdi, I. Szilágyi, S. Dóbé, *SCOUT-O3 Second Annual Meeting*, Jülich, 2006 március 20-24 (poszter).

8. OH formation in the gas-phase elementary reactions of CH_3CO and C_2H_5CO radicals with O_2, R. Nádasdi, I. Szilágyi, Gg. Kovács, J. Zádor and S. Dóbé, *BME Doktoráns Konferencia*, Budapest, 2008 február 8, (poszter).

9. UV absorption spectrum and photolysis quantum yield for methyl-ethyl-ketone, G. L. Zügner, R. Nádasdi, M. Farkas and S. Dóbé, *BME Doktoráns Konferencia*, Budapest, 2008 február 8, (poszter).

10. Photolysis quantum yield and OH reaction rate constant for methyl-ethyl-ketone, R. Nádasdi, G. L. Zügner, I. Szilágyi, S. Dóbé, E. Szabó, A. Tomas and C. Fittschen, *20th International Symposium on Gas Kinetics*, Manchester, 2008 július 20-25, (poszter).

11. Kinetics and mechanism of the reactions of C_2H_5CO and $CH_3CHC(O)H$ radicals with O_2, X. Song, B. Wang, I. Szilágyi, R. Nádasdi, J. Zádor and S. Dóbé, *20th International Symposium on Gas Kinetics*, Manchester, 2008 július 20-25, (poszter).

Other presentations

12. Absolute rate constants for the reactions of OH radicals with fluoro-alcohols and acetyl-fluoride, Gg. Kovács, I. Szilágyi, R. Nádasdi, S. Dóbé, T. Bérces, F. Márta, *19th International Symposium on Gas Kinetics*, Orleans, 2006 július 22-27, (poszter).

13. Competitive bromination kinetic study of C_2H_6, CH_2ClBr and neo-C_5H_{12}. Reaction kinetics and thermochemical implications, R. Nádasdi, I. Szilágyi, J. Zádor, G. Zügner, S. Dóbé, T. Bérces, F. Márta, *Third European Combustion Meeting*, Chania, Crete, 2007 április 11-13, (poszter).

14. Benzene photolysis at 254 nm in an atmospheric simulation chamber, E. Szabo, A. Tomas, C. Fittschen, P. Coddeville, R. Nadasdi, S. Dobe, *20th International Symposium on Gas Kinetics*, Manchester, 2008 július 20-25, (poszter).

15. Direct and Relative-Rate Kinetic Parameters and Thermochemistry of the Reaction of Br Atoms with CH_2ClBr, I. Szilágyi, D. Sarzynski, R. Nádasdi, G. L. Zügner, I. Fejes, S. Dóbé, *Austrian - Croatian - Hungarian Combustion Meeting*, Sopron, 2008 október 3, (poszter).